doi: 10.4149/gpb_2022004

Segmental flexibility of spectrin reflects erythrocyte membrane deformability

Ivan T. Ivanov and Boyana K. Paarvanova

Department of Physics, Biophysics, Roentgenology and Radiology, Medical Faculty, Thracian University, Stara Zagora, Bulgaria

Abstract. The frequency-dependent contribution of spectrin, the main cytoskeletal protein of red blood cell (RBC) membrane, to the complex admittance and capacitance of suspended RBCs have revealed two dielectric relaxations, β_{sp} (1.4 MHz) and $\gamma 1_{sp}$ (7 MHz). The strength of these relaxations was related to the ability of RBC membrane to deform. In this study the two relaxations were inhibited by N-ethylmaleimide (up to 5 mM), known to impair the RBC deformability, and the degree of inhibition, i.e., the number of accessible SH-groups on spectrin, depended on the deformation of RBC membrane. Dithiothreitol (up to 5 mM), which does not affect RBC deformability, did not affect the above dielectric relaxations in line with the absence of S-S groups on spectrin. Phenylhydrazine (up to 3 mM) and hydrogen hydroperoxide (up to 450 μM) are known to denature the haemoglobin of RBCs producing nanoparticles (globins) that bind to spectrin turning the RBC membrane rigid. At the same concentrations they were shown to inhibit progressively the two relaxations on spectrin. The results are in line with the involvement of some globin-sized segments of spectrin in the dielectric activity of spectrin and in the ability of RBC plasma membrane to deform.

Key words: Erythrocyte membrane — Dielectric relaxation — Spectrin segments — SH group exposure — RBC deformability

Abbreviations: DTT, dithiothreitol; EIS, electrochemical impedance spectroscopy; f, frequency of alternating electric field; f_c, characteristic frequency of dielectric relaxation; $f_{\beta sp}$, characteristic frequency of β_{sp} relaxation on MS spectrin; $f_{\gamma 1 sp}$, characteristic frequency of $\gamma 1_{sp}$ relaxation on MS spectrin; MS, spectrin-based membrane skeleton; NEM, N-ethylmaleimide; PHZ, phenylhydrazine; RBC, red blood cell; T_A, denaturation temperature of spectrin.

Introduction

The red blood cells (RBCs) are extremely elastic and deformable cells to supply human tissues with oxygen and dispose carbon dioxide. The mechanical properties of RBCs are strongly influenced by the mechanical function of their plasma membrane. The latter represents a membrane-skeleton complex containing lipid bilayer with intercalated proteins, mainly band 3 and glycophorin C, supported by under-membrane skeleton (MS) based on the long elastic filamentous protein spectrin. The spectrin filaments are constructed from tetrameric associations of two, α- and β-, heterodimer chains in head-to-head binding. In addition to spectrin-lipid interaction, the band 3-spectrin and the glycophorin C-spectrin bridges constitute the two major protein tethers that attach the spectrin skeleton to the lipid membrane (de Oliveira and Saldanha 2010). Both experimental and theoretical studies indicate a critical role for the spectrin-based skeletal network in general, and spectrin fila-

Correspondence to: Ivan T. Ivanov, Department of Physics and Biophysics, Medical Faculty of Thracian University, Stara Zagora 6000, Bulgaria
E-mail: ivanov_it@gbg.bg

ments in particular, in determining membrane deformability and elasticity, however, the precise mechanism remains uncertain (Mohandas et al. 1983; Sheetz 1983; Mohandas and Gallagher 2008). An important structural feature of spectrin dimer is the succession of 36 triple-helical spectrin repeats of about 106 amino acid residues, 20 in α-spectrin and 16 in β-spectrin. Both the stability of these repeat units and the dimer-dimer interaction are not static, but dynamic in the sense that they change reversibly under tensile forces imposed by the deformation of RBC, and indeed oscillate continuously between the open and closed states.

Electrochemical impedance spectroscopy (EIS) is a non-destructive method with high sensitivity for the changes at interfaces and membranes (Macdonald and Johnson 2005; Batyuk and Kizilova 2018). Recently a special EIS approach, differential thermal dielectroscopy at the denaturation temperature of spectrin, T_A, has been used to derive and test the dielectric activity of spectrin-based membrane skeleton of RBCs (Ivanov and Paarvanova 2019a, 2021). Two dielectric relaxations on the MS spectrin, termed β_{sp} (1.4 MHz) and $\gamma 1_{sp}$ (7 MHz) relaxations, were detected and described quantitatively using model approximation. Prior to testing the RBCs have been treated by a number of factors and conditions (alkaline pH, diamide, glutaraldehyde, wheat germ agglutinin, hypertonic media, metabolic starvation etc.) frequently used to sever either attachment site and reduce the deformability and flicker of RBC membrane. The general conclusion was that the strength of either relaxation was reduced by specific MS/lipid bilayer uncoupling while the inhibition of predominantly β_{sp} relaxation was related to the impairment of RBC deformability.

In this study, the indicated EIS approach was further used to investigate the relation between the dielectric activity of spectrin and mechanical function of human RBC membrane. The used SH-reagents indicated the exposure of spectrin SH-groups upon deformation of RBCs. Special attention was paid to chemical agents generating intracellular nanoparticles (globins of denatured hemoglobin), known to adhere specifically to spectrin filaments and impair the deformability of RBC plasma membrane. The obtained results indicate that the formed spectrin-globin complexes inhibit the dielectric activity of cytoskeletal spectrin in support of the view that segmental mobility of spectrin is important for the mechanical function of RBC plasma membrane.

Materials and Methods

Materials

Dithiothreitol (DTT), N-ethylmaleimide (NEM), phenylhydrazine (PHZ), H_2O_2, saponin S, digitonin, NaCl, mannitol, phosphate buffer and $MgCl_2$ were purchased from Sigma Chemicals Co., St. Louis, MO, USA.

RBCs and RBC ghost membranes

Human RBCs were isolated from freshly drawn blood samples, washed in a solution of 10 mM NaCl and 280 mM mannitol (further called working medium) and RBC ghost membranes were prepared as described previously (Ivanov and Paarvanova 2021).

Thermal dielectroscopy of RBC suspensions

Prior to test the RBCs at T_A temperature, they were suspended in the working medium (hematocrit 0.45). 70 μl of the suspension was introduced with a syringe into the working conductometric cuvette (conductometric constant, K = 6.5 cm^{-1}) that in turn was inserted into a hole of an aluminium block. After thermal equilibrium the block was heated with constant heating rate (1.5°C/min) across a temperature interval about T_A in order to derive the dielectric contribution of spectrin network. During the heating, the complex admittance, $Y^* = Y' + j.Y''$, and complex capacitance, $C^* = C' - j.C''$, were continuously measured and separated into their real (Y', C') and imaginary (Y'', C'') parts using Solartron 1260 Impedance Frequency Analyzer (Schlumberger Instruments, Hampshire, England) controlled by a computer. Here, j is the imaginary unit, $j^2 = -1$. The values of Y^* and C^* were measured at 16 frequencies between 30 kHz and 15 MHz, and scanned sequentially with an integration time of 1 s. The static (low frequency) capacitance, C_0, of tested RBC suspensions, determining the static capacitance of RBC plasma membrane, was obtained by extrapolation of the values determined within the frequency interval of 30–200 kHz. The experimental setup, designed to collect the raw thermal dielectroscopy data was shown previously (Ivanov and Paarvanova 2021).

RBC modification by stress-inducing agents

The washed RBCs were tested at T_A either as control ones or after alteration by stress-inducing agents. To minimize the degradation of these reagents, their solutions were prepared immediately prior to test heating.

To modify the disulphides of RBC plasma membranes, the washed RBCs were suspended at hematocrit 0.10 in working media containing DTT with the indicated concentration. To modify the thiol groups of MS spectrin, the RBCs were suspended at hematocrit 0.10 in media containing the indicated concentration of NEM, 10 mM NaCl and indicated concentration of mannitol in order to achieve the desired equilibration volume of RBCs. After incubation at room temperature for 50 min to complete the reaction, the

modified RBCs were isolated, suspended in the working medium, hematocrit 0.45 and subjected to test heating across T_A temperature.

To incorporate saponin S in the lipid bilayer, 150 µl RBCs were suspended in 1 ml isotonic medium of 30 mM NaCl, 240 mM mannitol (an analogue to sucrose), 2 mM Mg^{2+} and saponin S at the indicated concentrations. After 15 min incubation at room temperature the cells were isolated without traces of hemolysis, re-suspended in the same medium without saponin, hematocrit 0.45, and subjected to test heating across T_A to derive the dielectric contribution of spectrin network.

To accomplish modification by PHZ, 0.1 ml RBCs were incubated in 0.9 ml working medium, containing PHZ at the indicated concentration, at room temperature for 30 min. The modified cells were isolated, washed and suspended in working medium without PHZ, hematocrit 0.45, and tested at the T_A temperature.

To accomplish modification by H_2O_2, the washed RBCs were adjusted to a hematocrit of 0.10 in working medium, containing the indicated concentration of H_2O_2, at room temperature for 40 min. The RBCs were exposed to H_2O_2 for less than one hour in order to avoid the alteration of the lipid bilayer as the action of H_2O_2 within the first hour is mainly related to the membrane skeleton (Hale et al. 2011). The modified cells were isolated, washed with H_2O_2, suspended in working medium, hematocrit 0.45, and tested at the T_A temperature.

Results

Spectrin contribution to the dielectric properties of RBC plasma membrane

It is generally accepted that the dielectric properties (conductance, capacitance) of RBC plasma membrane are chiefly determined by the lipid membrane and its small width (~7 nm). The idea to define such contribution is based on the conception that spectrin network is well separated from the lipid membrane and its impact to latter is transmitted mainly through the long (30 nm) attachment bridges. At the denaturation temperature of spectrin, T_A (49.5°C, projected to zero heating rate) (Brandts et al. 1977), the dimers of cytoskeletal spectrin dissociate into α- and β-subunits with eventual aggregation of the denatured β-subunits (Yoshino and Minari 1987). Consequently, the dielectric activity of spectrin and its impact on the lipid membrane were assumed quenched. Indeed, spectrin denaturation resulted in huge sigmoid and frequency-dependent changes in *Y'*, *Y"*, *C'* and *C"* taking place within the temperature interval of about 6°C around T_A (Ivanov and Paarvanova 2016). Each change was defined as the value at the native minus the value at the denatured state of spectrin, respectively. However, in addition to the main component, related to the powerful spectrin denaturation, each apparent change contained a small component due to the combined effect of temperature on a multitude of processes involving the suspension medium and cytosol. Compared to the former, the latter component was small and linear because it was not caused by the denaturation of a protein and arose within a relatively short temperature interval. Hence, it was determined for an equivalent temperature interval prior to spectrin denaturation and subtracted from the apparent changes in Y^* and C^* at T_A (Ivanov et al. 2020; Ivanov and Paarvanova 2021). This procedure extracted the spectrin-linked portion of the dielectric changes at T_A. At each frequency the extracted, spectrin-linked changes in the dielectric properties of RBC suspension at T_A are further noted as $\Delta Y'(f)$, $\Delta Y''(f)$, $\Delta C'(f)$ and $\Delta C''(f)$.

As previously reported, the $\Delta Y'(f)$, $\Delta Y''(f)$, $\Delta C'(f)$ and $C''(f)$ changes at T_A were almost identical when obtained with suspensions of either fresh RBCs or their isolated RBC ghost membranes, resealed with 75 mM NaCl. This finding, combined with the elimination of the impact of all accompanying processes, indicate that these changes were dominated chiefly by the denaturation of the major cytoskeletal protein spectrin and subsequent threshold alteration of the plasma membrane. Based on the assumption that the dielectric activity of denatured spectrin is nil within the frequency interval from 30 kHz to 15 MHz, above mentioned dielectric changes were assumed to represent the contribution of native MS spectrin to the dielectric properties of plasma membranes just prior to the T_A. The dielectric contribution of MS spectrin was studied using the $\Delta Y''$ *vs.* $\Delta Y'$ and $\Delta C''$ *vs.* $\Delta C'$ plots, representing the complex plane plots of spectrin-linked portions of the electric admittance and capacitance of RBCs (exemplified by the Figs. 1C and 2C).

Graphical and model representation of the dielectric relaxations on MS spectrin

The presence of two perfect semicircle arcs on the $\Delta Y''$ *vs.* $\Delta Y'$ plot (Fig. 1C) has been attributed to two dielectric relaxations on MS spectrin network (Ivanov et al. 2020; Ivanov and Paarvanova 2021). The upper semicircle arc expressed the β_{sp} relaxation of spectrin explained as piezo effect on spectrin, powered by the electrostriction of the lipid bilayer during the build-up of charges on its two sides. The same electrostriction has been extensively used in the black lipid bilayer preparations to expel the remaining organic solvent. The lower semicircle arc revealed the $\gamma 1_{sp}$ relaxation (natural oscillations of spectrin dipoles) whose characteristic frequency, f_c, has been shown decreased by glycerol and increased at higher concentrations of the ions in cytosol (Ivanov and Paarvanova 2016).

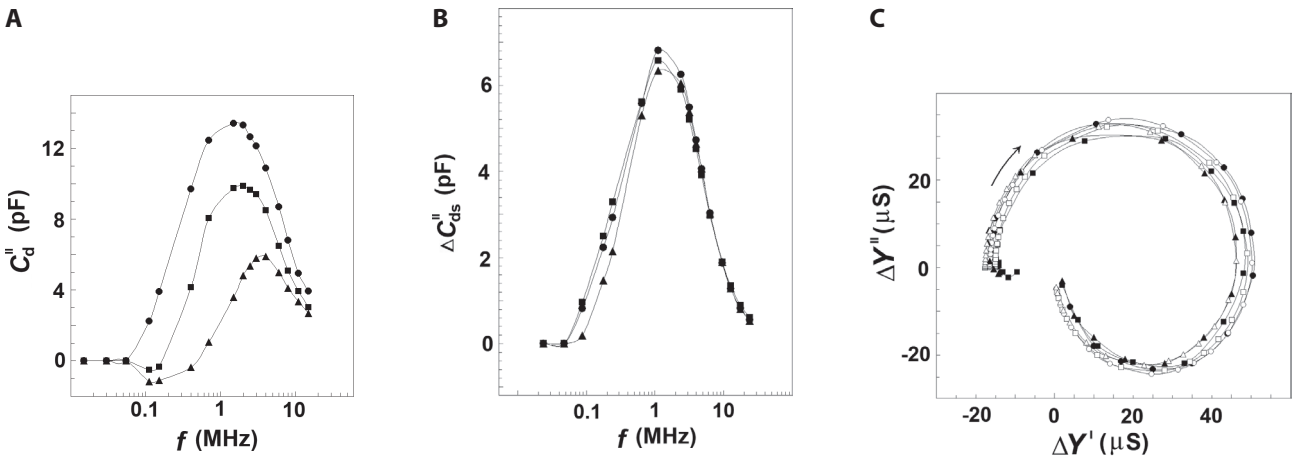

Figure 1. Effect produced by the DTT-treatment of RBCs on the dielectric behaviour of their plasma membranes. **A.** Dielectric loss curve of RBC plasma membranes. The dielectric loss at 37°C of the plasma membrane of RBCs, C_d" (pF), is plotted against the frequency, f (MHz). **B.** Dielectric loss curve of MS spectrin. The dielectric loss at 47°C of MS spectrin, ΔC_{ds}" (pF), is plotted against the frequency, f (MHz). **C.** Plot of spectrin-linked portion of the complex admittance. The corrected changes at T_A in imaginary admittance, ΔY" (μS), are plotted against the corrected changes at T_A in real admittance, ΔY' (μS), expressed with full symbols. Curved arrow indicates the increase in frequency from 30 kHz to 15 MHz. Open symbols indicate the respective model plot, *y" vs. y'*, obtained as explained in the text. The tested suspension contained control RBCs (●, ○) and RBCs pre-treated by DTT at concentrations 1 mM (▪, □) and 5 mM (▲, Δ). The RBCs were suspended in working medium at hematocrit of 0.45 and heated (heating rate of 1.5°C/min) across the T_A temperature to derive the dielectric contribution of spectrin network. This and next figures represent the typical result out of at least three experiments.

In this study, the β_{sp} and $\gamma1_{sp}$ relaxations on MS spectrin were modelled by an appropriate equivalent electric circuit as described recently (Ivanov et al. 2020; Ivanov and Paarvanova 2021). The model representation was used to better differentiate the two relaxations and describe them by quantitative parameters. The basic part of the model contained a capacitor and resistor, connected in series, whose admittance plot represents a semicircle arc frequently used to express a single-time dielectric relaxation. The model contained two such circuits, connected in parallel, each one representing different relaxation. The model parameters, $R_{\beta sp} = 1/Y_{\beta sp}$ and $C_{\beta sp}$, of the upper circuit represented the best fit values for the β_{sp} relaxation, while the $R_{\gamma 1sp} = 1/Y_{\gamma 1sp}$ and $C_{\gamma 1sp}$ of the lower circuit were the best fit values for the $\gamma1_{sp}$ relaxation. Using the experimental data and the measured characteristic frequencies of the two relaxations, $f_{\beta sp}$ and $f_{\gamma 1sp}$, the initial approximate values of all capacitive and resistive elements were calculated. Next, they were adjusted by several iteration steps resulting in good enough fit of the admittance plot of model circuit to the experimentally obtained plot as shown in Figure 1C (open circles) and in Table 1. The strengths of β_{sp} and $\gamma1_{sp}$ relaxation, $Y_{\beta sp}$, and $Y_{\gamma 1sp}$, respectively, were represented by the apparent radiuses of respective semicircles in Figure 1C.

It has been assumed that the energy dissipation ratio, $-Y_{\gamma 1sp}/Y_{\beta sp}$, and charge accumulation ratio, $-C_{\gamma 1sp}/C_{\beta sp}$, represent the amount of dissipated energy and stored charges, respectively, on MS spectrin during the $\gamma1_{sp}$ relaxation relative to that in β_{sp} relaxation. In previous studies (Ivanov and Paarvanova 2019a, 2019b), the $-Y_{\gamma 1sp}/Y_{\beta sp}$ ratio (~ 0.85 in control RBCs) has been shown to decrease on disturbing the spectrin-band 3 attachment site and in the presence of aprotic solvents while it increased on disturbing the spectrin-actin interaction and in the presence of protic solvents. In fresh

Table 1. Model parameters of β_{sp} and $\gamma1_{sp}$ dielectric relaxations on the MS spectrin of RBCs, pre-treated by DTT

DTT (mM)	C_0 (pF)	Y_0 (μS)	$-Y_{\beta sp}$ (μS)	$-C_{\beta sp}$ (pF)	$Y_{\gamma 1sp}$ (μS)	$C_{\gamma 1sp}$ (pF)	$-Y_{\gamma 1sp}/Y_{\beta sp}$	$-C_{\gamma 1sp}/C_{\beta sp}$
0	45	74	87	15.4	70	1.4	0.805	0.091
1	42	91	86	14.8	72	1.4	0.83	0.096
5	39	110	84.6	14.5	69	1.3	0.815	0.089

C_0 and Y_0 are the static (low frequency) capacitance and conductance, respectively, of tested RBC suspension. The modified cells were tested at T_A in the working medium. Other details as for Figure 1.

RBCs, the charge storage ratio, $-C_{\gamma 1sp}/C_{\beta sp}$, is low (~ 0.13) in line with the high efficiency for charge generation of the piezo effect during the β_{sp} relaxation (Ivanov et al. 2020).

Dielectric loss curve of MS spectrin in radio-frequency range

At a given temperature, the dissipation, *C*", of the tested RBC suspension represents the rate at which the electric field energy is dissipated due to conduction of ions and oscillation of electric dipoles (Gabriel et al. 1996). The conduction loss strongly prevails at low frequencies and decreases with the reciprocal of the frequency, *f*. At the radio-frequency range it becomes smaller than the dielectric loss as the latter peaks up at the relaxation frequency of dipoles. Thus, log(*C*") obeys a characteristic frequency dependence which allows the discrimination of both types of energy loss on the frequency domain. For human blood at frequencies between 10 Hz and 0.1 MHz, the dielectric loss is negligible in respect to conduction loss and the log(*C*") linearly declines with log*(f)* (Gabriel et al. 1996). Above 0.1 MHz the linear shape of the log(*C*")/log*(f)* dependence is disturbed as the latter represents mainly the energy loss due to dipole relaxation. Above considerations allowed separate determination of the two types of energy loss.

The values of C"*(f),* measured with a given suspension at a given temperature within the low frequency portion (30–50 kHz for intact RBCs and 50–100 kHz for modified RBCs), were used to obtain an approximate analytical (e.g. power law) expression for the conduction loss. The obtained analytical expression was assumed to represent the pure conduction loss both at low and high frequencies. For the radio-frequency range (0.1–15 MHz), conduction loss data, calculated from this expression, were subtracted from the experimentally measured values of C"*(f)* allowing the remainder to be defined as dielectric loss curve, C_d"*(f)*, of tested suspension at the chosen temperature (exemplified by Fig. 1A) (Ivanov et al. 2020).

The dielectric loss of a RBC suspension is represented by the total area under the loss curve, C_d"*(f)*, shown in Figure 1A. Concerning a general system, this area is proportional to the total amount of dipoles and their dipole moments, irrespective of the spatial distribution of dipoles (Pethig 1979). The radio frequency loss curve, obtained with suspensions of RBC ghost membranes, resealed with 75 mM NaCl, practically coincided to that of the suspensions of parent RBCs (data not shown). This coincidence happened because over much of the frequency interval, where hemoglobin absorbs (Simeonova et al. 2002), the field was not able to see the cytosole and the two loss curves reflected mainly the powerful radio-frequency (beta) relaxation of RBC plasma membrane. Hence, the C_d"*(f)* curve of RBC suspensions was assumed to reflect mainly the dielectric loss profile of RBC plasma membranes.

Using either whole human blood or human blood, thinned out by isotonic NaCl saline, and another way for the removal of conduction loss other investigators (Gabriel et al. 1996; Desouky 2009; Abdalla et al. 2010; Abdalla 2011) have obtained similar bell-shaped dielectric loss curve with a peak centered at about 1.3 MHz. The origin of this energy absorption curve has been assumed related to a resonance of the incident field with some natural high-frequency oscillations of the blood particles, mainly RBCs (Gabriel et al. 1996; Abdalla 2011). In our studies the dielectric loss curve, C_d"*(f)*, of tested RBCs at temperatures up to 48°C had more complicated shape (see Fig. 1A) and was assumed to represent a convolution of several energy absorptions (Ivanov and Paarvanova 2020). Using the heat denaturation of spectrin, one of these absorptions was resolved and ascribed to the dielectric loss on spectrin network as explained next.

The frequency profile of the dielectric loss curve of RBC suspensions practically did not change within the temperature intervals of 30–47°C and 53–59°C. However, it abruptly changed at T_A, indicating substantial drop of dielectric loss due to the denaturation of spectrin. To obtain the dielectric loss curve of MS spectrin, ΔC_{ds}"*(f)*, the dielectric loss curve of RBC suspension, C_d"*(f)*, at 53°C was subtracted from that at 47°C and the result (exemplified by Fig. 1B) was corrected by temperature using the dielectric loss curve at 41°C (Ivanov et al. 2020). The dielectric loss curve of spectrin, ΔC_{ds}", was obtained using differential and temperature corrected values that fully eliminated the contribution of the dielectric loss of cytosolic proteins, mainly that of hemoglobin at 1 MHz (Simeonova et al. 2002). Hence, identical dielectric loss curves for MS spectrin were obtained using either suspensions of RBC ghost membranes, resealed with 75 mM NaCl, or suspensions of parent RBCs.

The dielectric loss curve of spectrin, ΔC_{ds}"*(f)*, showed the frequency profile of the electric energy spent on MS spectrin mainly during the β_{sp} relaxation (Ivanov and Paarvanova 2019a). In addition, an almost indistinguishable weak peak, presumably related to the $\gamma 1_{sp}$ relaxation, was seen on the high frequency end of this curve. Similar to the ΔC_{ds}"*(f)* curve, the ΔC" *vs.* ΔC' plot (Fig. 2C) showed a well-defined semi-circle, corresponding to the β_{sp} relaxation, with a slight bulge on its high frequency end corresponding to the $\gamma 1_{sp}$ relaxation (Ivanov and Paarvanova 2019a). Both the β_{sp} and $\gamma 1_{sp}$ relaxations were, however, perfectly resolved on the ΔY" *vs.* ΔY' plot of spectrin-linked portion of the electric admittance of RBCs (Fig. 1C).

Effect of membrane permeable sulfhydryl reagents on the dielectric relaxations of MS spectrin

DTT is particularly strong reducing reagent cleaving the accessible disulfide bonds between cysteine amino acids

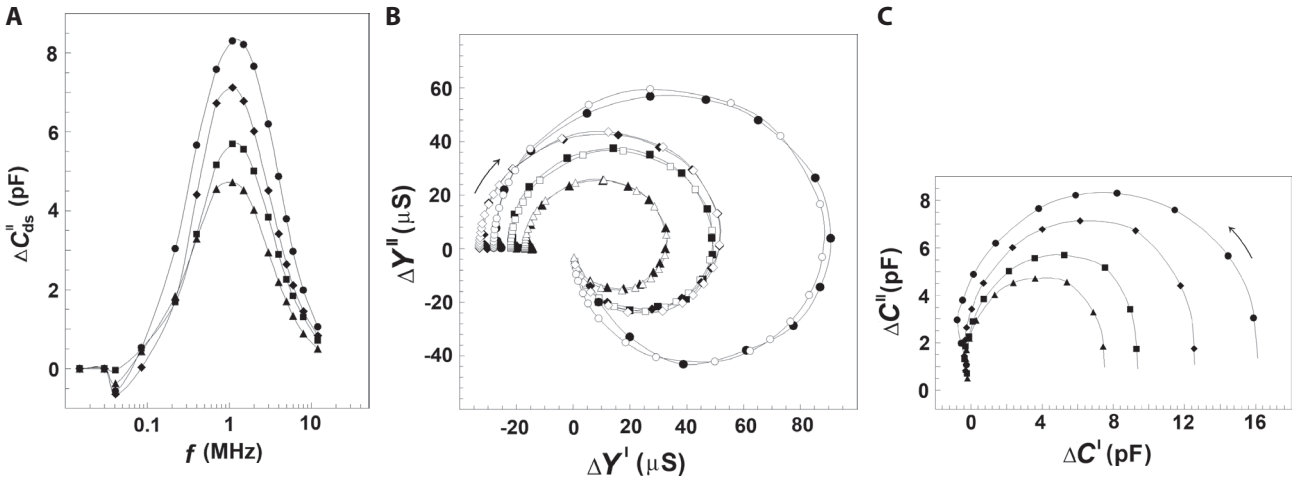

Figure 2. Effect produced by the osmotically-induced volume changes in RBCs on the accessibility to NEM of SH-groups of MS spectrin. **A.** Dielectric loss curve of the MS spectrin. **B.** Plot of spectrin-linked portion of the complex admittance of RBCs. **C.** Plot of spectrin-linked portion of the complex capacitance of RBCs. The dielectric loss of MS spectrin, ΔC_{ds}" (pF), is plotted against the corrected changes at T_A in real capacitance, ΔC ' (pF). The tested suspension contained RBCs pre-treated by 0 mM NEM in isotonic medium of 10 mM NaCl and 280 mM mannitol (●, ○) and RBCs pre-treated by 1 mM NEM in media containing 10 mM NaCl and mannitol at concentrations 280 mM (▪, □), 180 mM (▲, Δ) and 580 mM (◊, ♦). Other details as for Figure 1.

in proteins. NEM forms stable, covalent thioether bonds with sulfhydryl groups of proteins, enabling them to be permanently blocked to prevent disulfide bond formation. The application of the two sulfhydryl reagents in this study was substantiated based on their specific reactivity and different effects they produce on the deformability of RBC plasma membrane.

Effect of DTT

Figure 1A shows the effect of DTT-treatment of RBCs on the dielectric loss curve of their plasma membranes. As with intact RBCs, this curve practically did not alter its shape when obtained either at 47°C or at lower temperatures, for example at 37°C (not shown). Compared to intact RBCs, the dielectric loss curve of the plasma membranes of DTT-treated RBCs was specifically modified. With 1 mM DTT, the dielectric loss within the 1–10 MHz interval was slightly decreased, while that at the low-frequency end (30–200 kHz) was totally removed. Using higher concentrations of DTT (2 and 5 mM), the dielectric loss within the 1–10 MHz interval was further decreased, while the low-frequency interval with no dielectric loss became substantially broader. This strong modification of the loss curve indicates that DTT reacted with some membrane proteins changing their conformation that caused decrease in the energy absorption especially in the low-frequency interval.

While DTT strongly modified the loss curve of RBC plasma membrane it was unable to affect the dielectric behavior of spectrin network. This is demonstrated in Figure 1B and C that show the dielectric loss curve of MS spectrin, ΔC_{ds}", and the plot of spectrin-linked portion of the electric admittance of RBCs, ΔY" *vs*. ΔY', respectively, of DTT-treated RBCs. Figure 1B and C and Table 1 substantiate that, up to the concentrations of 5 mM, DTT did not affect the dielectric behavior of MS spectrin despite the strong effect it inflicted on the plasma membrane. Considering the reports that DTT-treatment of RBCs does not alter their deformability (Almeida et al. 2008; Sheremet'ev and Sheremet'eva 2009; Saldanha et al. 2010), the results shown in Figure 1B and C support the recent findings (Ivanov and Paarvanova 2021) that the ability of many agents to inhibit the dielectric activity of RBC spectrin network correlates their ability to impair the deformability of RBC plasma membrane.

The results, shown in Figure 1A, B and C could be explained based on the reports that most of the integral proteins (excluding the major glycophorin C) contain disulfide bonds, accessible to DTT, while there is no evidence to suggest that native MS spectrin dimer contains disulfide bonds (Speicher et al. 1983; Becker et al. 1986). These results possibly indicate that DTT left the spectrin filaments intact while it cleaved the accessible disulfide bonds between cysteine residues of some integral proteins. The above-mentioned elimination of the dielectric loss within the low-frequency interval persisted when the loss curves prior to and after the spectrin denaturation were compared (not shown). This indicates the involvement of a membrane protein(s) with greater thermal stability than spectrin.

Effect of NEM

The spectrin filaments of RBC plasma membrane contain substantial number of thiol groups with different accessibility to various thiol reagents. There is evidence that chemical modification of thiol groups in spectrin affects the structure and stability of RBC cytoskeleton and the deformability and stability of RBC (Fischer et al. 1978; Becker et al. 1986; Chasis and Mohandas 1986; Rangachari et al. 1989; Go et al. 2015; Barbarino et al. 2020). After modification of about 20% of the SH-groups of RBC plasma membrane the monofunctional SH-reagent NEM has been shown to decrease twice the RBC deformability (Fischer et al. 1978). Another study (Chasis and Mohandas 1986) reported that treatment of RBC by NEM, at the same conditions as those applied in this study, have reduced the deformability of RBCs two-folds. The authors (Becker et al. 1986) assume that NEM and other monofunctional agents reduce RBC deformability *via* spectrin, for instance by impeding changes of angles in the protein chain.

The treatment by 1 mM NEM of RBCs, when they were suspended in the working medium of 300 mOsm, which is isotonic to RBC cytosol, resulted in about 40–50% inhibition of both the dielectric loss curve (Fig. 2A) and the strength of β_{sp} relaxation (Fig. 2B,C; Table 2) on their spectrin network. This extent of inhibition is comparable to the known impairment of RBC membrane deformability (Fischer et al. 1978; Becker et al. 1986; Chasis and Mohandas 1986). Taking into account the published data that NEM-treatment reduces the deformability of RBCs, the results shown in Figure 2 and Table 2 represent additional prove of the claim (Ivanov and Paarvanova 2021) that the ability of many agents to inhibit the dielectric activity of RBC spectrin network correlates their ability to impair the deformability of RBC plasma membrane.

Recent reports have demonstrated that some buried cysteines of spectrin filaments became exposed to thiol reagents when the RBCs were mechanically stressed (Johnson et al. 2007). Once the deformation of RBC has been shown to expose additional cysteines on spectrin one should expect it could modulate the effect of NEM on the dielectric activity of spectrin. In this study, this possibility was probed with RBCs, which were deformed by changing their volume and shape. Aiming at this, the NEM was applied on RBCs when they were either shrunk in a hypertonic medium of 600 mOsm or sub-critically swelled in a hypotonic medium of 200 mOsm. The results, obtained with 1 mM NEM, are shown in Figure 2A, B and C and Table 2. Similar results were obtained with 5 mM NEM (not shown).

Compared to the isotonic medium, the dielectric activity of spectrin was stronger inhibited by NEM when RBCs were swelled at 200 mOsm and less inhibited in case the RBCs were shrunk at 600 mOsm. In general, the binding of NEM to the accessible thiol groups of spectrin would produce stronger inhibition in case the number of these groups is greater and *vice versa*. Thus, the obtained results are in line with the view that in case the RBC plasma membrane was isotropically stretched the underlying spectrin filaments exposed additional thiol groups while in case of isotropic shrinkage a part of accessible thiol groups became buried. The results support the conclusion that dielectric activity of spectrin in radiofrequency region reflects the spectrin intramolecular mobility provided that NEM reduce both, for instance by impeding the changes of angles in the protein chain.

On the other hand, the modification of RBCs by NEM strongly reduced the static capacitance and moderately increased the low frequency conductance of RBC plasma membranes (Table 2). These outcomes did not depend on whether NEM was applied on either intact cells or cells subjected to swelling and shrinkage (Table 2). These findings are consistent to the view that both RBC membrane capacitance and conductance mainly depend on the lipid membrane and its modification.

Comparing the values of $-Y_{\gamma 1sp}/Y_{\beta sp}$ and $-C_{\gamma 1sp}/C_{\beta sp}$ for intact RBCs with these for NEM-treated RBCs (Table 2), it could be concluded that NEM produced stronger inhibition of $\gamma 1_{sp}$ relaxation, compared to β_{sp} relaxation on MS spectrin. This finding has been already published (Ivanov and Paarvanova 2019a) and explained by the known ability of NEM to weaken the band 3-spectrin attachment site (Blanc et al. 2010). Furthermore, the values of $-Y_{\gamma 1sp}/Y_{\beta sp}$ and $-C_{\gamma 1sp}/C_{\beta sp}$ were much stronger reduced with shrunk cells, compared to intact and swelled ones. This is due to the

Table 2. Model parameters of β_{sp} and $\gamma 1_{sp}$ dielectric relaxations on the MS spectrin of RBCs, pre-treated by NEM in media with indicated osmotic pressure π, inducing osmotic changes in RBC volume

NEM (mM)	π (mOsm)	Y_0 (μS)	C_0 (pF)	$-Y_{\beta sp}$ (μS)	$-C_{\beta sp}$ (pF)	$Y_{\gamma 1sp}$ (μS)	$C_{\gamma 1sp}$ (pF)	$-Y_{\gamma 1sp}/Y_{\beta sp}$	$-C_{\gamma 1sp}/C_{\beta sp}$
0	300	48	47	153	18.7	125	2.3	0.817	0.125
1	300	92	33	90	13.0	68	1.4	0.756	0.104
1	200	93	33	63	9.1	46	0.9	0.730	0.100
1	600	95	35	102	14.8	69	1.2	0.676	0.078

Other details as for Figure 2 and Table 1.

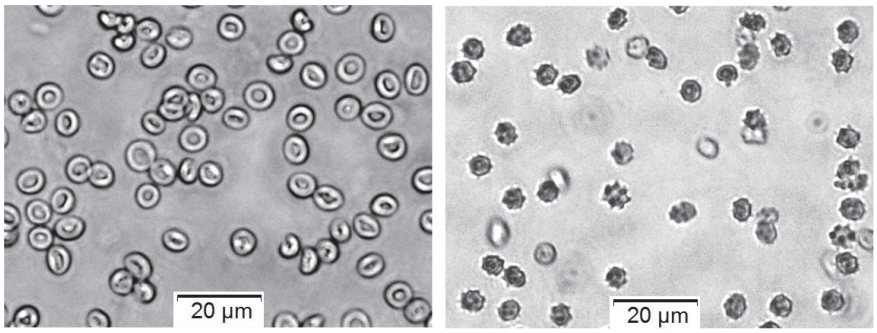

Figure 3. Micrographs of RBCs suspended in isotonic media of 30 mM and mannitol. Left: intact RBC, right: RBCs treated by saponin S (0.07 mg/ml) in isotonic medium of 30 mM NaCl and mannitol.

effect of mere RBC shrinkage (Ferru et al. 2011), additional and synergistic to that of NEM, both causing weakening of the band 3-spectrin attachment site.

Prelytic effect of saponin S and digitonin on the dielectric relaxations on the MS spectrin of RBCs

Saponins (saponin S and digitonin) are amphiphilic non-ionic surfactants known for their specific interaction with the lipid membrane of RBCs resulting in the formation of membrane barrier defects (Seeman et al. 1973; Francis et al. 2002). At the prelytic stage the saponins have been shown to alter the structure of the lipid bilayer by forming complexes with cholesterol and extracting it from the core of bilayer (Frenkel et al. 2014). Transmission electron microscopy has revealed the formation of uniformly distributed multilamellar stacks composed of crystallized lipids and pits with diameter of 4–5 nm that assumingly transformed into irreversible pores during the lytic stage (Sleep et al. 1999; Baumann et al. 2000).

At lytic concentrations saponin transforms the RBCs into smooth spherical ghost membranes indicating disruption of the membrane-skeleton interaction. During the lytic stage the saponin-induced permeabilization of RBC lipid bilayer has been shown to cause aggregation of band 3 and other transmembrane proteins, weakening the interaction between transmembrane proteins and the cytoskeleton and re-localization of associated proteins of the cytoskeleton (Baumann et al. 2000).

The resistance of RBCs against saponin-induced hemolysis has been shown to increase in isotonic media containing sucrose or glycine (Winter 1994). This finding was used here to incorporate greater amounts of saponin S in the lipid bilayer of RBC membrane without hemolysis.

The specific modification of RBC plasma membranes by saponin S produced irreversible change in the shape of cells from stomatocytes to spheroechinocytes (Fig. 3) indicating irreversible disturbance of the lipid membrane-cytoskeleton interactions. In line with previous studies (Baumann et al. 2000; Frenkel et al. 2014) the structure of the lipid membrane was strongly disturbed as evident by the marked increase in the conductance and decrease in the capacitance of RBC membrane (Table 3). Compared to the suspensions of control RBCs, the low frequency (1 kHz) conductance of the suspensions of RBCs, treated by 0.035 mg/ml (23 μM) saponin S, increased four times indicating strong permeabilization of RBC membranes. The conductometric estimation showed that prior to the spectrin denaturation the cells lost only about 5% of their content of inorganic ions (K^+, Cl^- and Na^+) and sustained osmotic shrinkage of similar extent. Nevertheless, the dielectric loss curve (Fig. 4A) and the strength of dielectric relaxations on MS spectrin (Fig. 4B and Table 3) were reduced about four times. Using saponin S with the concentration of 0.07 mg/ml (46 μM) the low frequency (1 kHz) conductance of RBC suspension and the loss of cytosolic ions proportionally increased nevertheless, the extent of inhibition of dielectric loss and dielectric relaxations remained as for the lower concentration (Fig. 4A,B and Table 3). Thus, the saponin S-treatment of RBC produced strong and threshold inhibition of the dielectric relaxations on spectrin network. Similar results were obtained using another type of saponin, digitonin (not shown).

Table 3. Model parameters of β_{sp} and $\gamma 1_{sp}$ dielectric relaxations on the MS spectrin of RBCs, pre-treated by saponin S

Saponin S (mg/ml)	C_0 (pF)	Y_0 (μS)	$-Y_{\beta sp}$ (μS)	$-C_{\beta sp}$ (pF)	$Y_{\gamma 1sp}$ (μS)	$C_{\gamma 1sp}$ (pF)	$-Y_{\gamma 1sp}/Y_{\beta sp}$	$-C_{\gamma 1sp}/C_{\beta sp}$
0	50	94	155	22.40	140	2.6	0.903	0.117
0.035	32	242	38	5.50	30	0.73	0.789	0.134
0.070	29.5	289	33.4	5.91	28	0.891	0.838	0.151

Other details as for Figure 4 and Table 1.

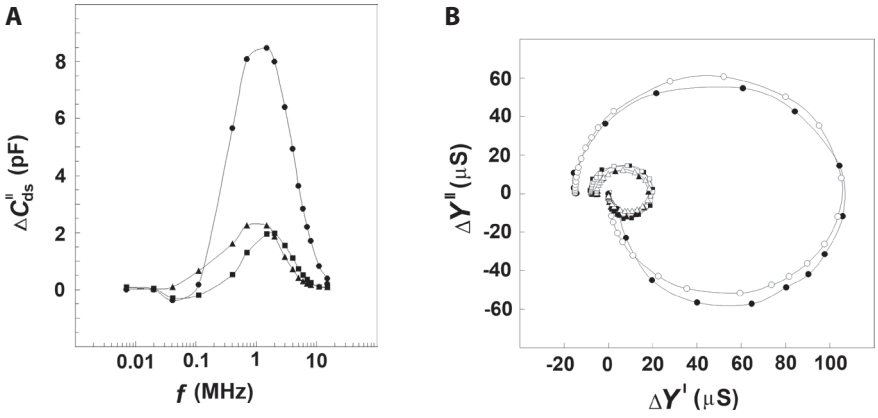

Figure 4. Effect of saponin S on the dielectric relaxations on the MS spectrin of RBCs. Dielectric loss curve of the MS spectrin (**A**) and plot of spectrin-linked portion of the complex admittance (**B**) of RBCs. Suspensions contained control RBCs (●, ○) and RBCs pre-treated by saponin at concentrations 0.035 mg/ml (▪, □) and 0.075 mg/ml (▲, Δ). The RBCs were suspended in isotonic medium of 30 mM NaCl and mannitol. Other details as for Figure 1.

According to the previous studies on RBCs (Ivanov and Paarvanova 2016, 2019a), the electrostriction of the lipid membrane and its coupling to the spectrin network have been considered as prerequisites for the appearance of β_{sp} and $\gamma 1_{sp}$ dielectric relaxations on skeletal spectrin. Under the impact of saponin, the strong disturbance of the lipid bilayer, as evidenced by its permeabilization and impaired ability to store charges, should inhibit its electrostriction while the aggregation of integral proteins, mainly band 3, should impair the coupling of lipid membrane to skeleton. Thus, the strong and threshold inhibition of dielectric relaxations on the spectrin of saponin-treated cells is in line with above claims.

Effect of the oxidative denaturation of hemoglobin on the dielectric relaxations of MS spectrin

Effect of PHZ

In vitro treatment of RBCs with PHZ results in alteration of MS spectrin network and decrease in the ability of RBCs to deform (Ramot et al 2008). PHZ oxidizes the main cytosolic protein, hemoglobin, precipitating free radical attack and denaturation of hemoglobin and damaging some membrane proteins in lesser extent. The alpha-hemoglobin chains (globins) of denatured hemoglobin selectively associate with the spectrin of membrane skeleton resulting in the formation of Heinz bodies and reduced RBC deformability (Ramot et al 2008). In addition to the aggregation of modified hemoglobin molecules to spectrin, the exposure of human RBCs to PHZ results in direct oxidative damage of MS spectrin (Arduini et al. 1989).

The results of Reinhart et al. (1986) indicate that the PHZ-induced oxidative damage of RBCs with discrete Heinz body formation causes focal membrane rigidification but does not affect the global cellular deformability until the Heinz bodies nearly cover the entire cell endoface.

Here, the effect of PHZ on RBC spectrin network was studied at experimental conditions (hematocrit value and PHZ concentrations) as those in other studies (Reinhart et al. 1986). Up to 3 mM, PHZ produced strong concentration-dependent inhibition of β_{sp} and $\gamma 1_{sp}$ relaxations, as shown in the ΔY" *vs.* ΔY' plot (Fig. 5B), and of β_{sp}

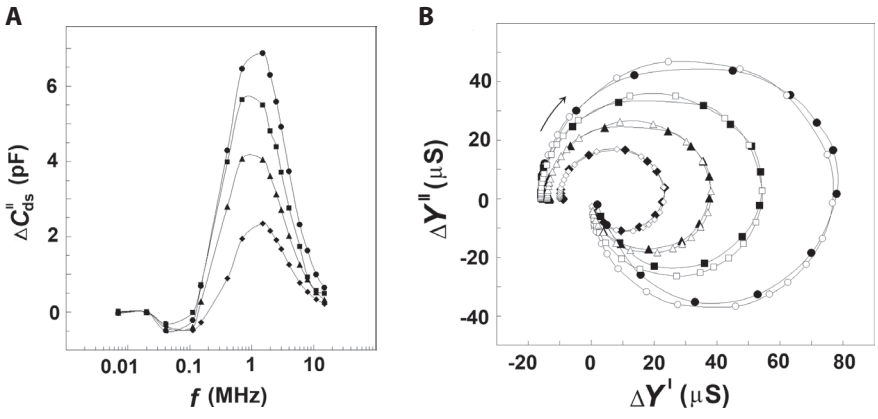

Figure 5. Effect of PHZ on the dielectric relaxations on the MS spectrin of RBCs. Dielectric loss curve of the MS spectrin (**A**) and plot of spectrin-linked portion of the complex admittance (**B**) of PHZ-treated RBCs. Suspension contained control RBCs (●, ○) and RBCs treated by PHZ at concentrations 1 mM (▪, □), 2 mM (▲, Δ) and 3 mM (♦, ◊). Other details as for Figure 1.

Table 4. Model parameters of β_{sp} and $\gamma 1_{sp}$ dielectric relaxations on the MS spectrin of RBCs, pre-treated by PHZ

PHZ (mM)	C_0 (pF)	Y_0 (μS)	$-Y_{\beta sp}$ (μS)	$-C_{\beta sp}$ (pF)	$Y_{\gamma 1sp}$ (μS)	$C_{\gamma 1sp}$ (pF)	$-Y_{\gamma 1sp}/Y_{\beta sp}$	$-C_{\gamma 1sp}/C_{\beta sp}$
0	37	71	124	14.1	108	1.9	0.871	0.135
1	36	85.5	88	14.0	72	1.4	0.818	0.102
2	35.2	96	61.9	11.0	48	0.8	0.775	0.078
3	34	96	41	5.9	31	0.5	0.756	0.092

Other details as for Figure 5 and Table 1.

relaxation, as shown in the plot of dielectric loss curve of MS spectrin (Fig. 5A).

Figure 5B (open circles) shows the obtained complex admittance plots of model electric circuit for each PHZ concentration. The respective capacitive and resistive elements of the model circuit (Table 4) represent quantitative estimation of the PHZ-induced inhibition of the two relaxations. Figure 5 and Table 4 substantiate that PHZ produced strong dose-dependent inhibition of the two dielectric relaxations at the same concentration range where, according to Reinhart et al. (1986), it produces dose-dependent stiffening effect on RBC plasma membrane.

In addition to the main inhibitory effect on dielectric relations, PHZ produced median by strength dose-dependent decrease in the $-Y_{\gamma 1sp}/Y_{\beta sp}$ ratio (Table 4), indicating disturbance of spectrin/band 3 attachment site. This outcome suggests the modification of other cytoskeletal proteins, in addition to spectrin, in the PHZ-induced alteration of RBC plasma membrane. The preservation of the values of static capacitance and conductance (Table 4) suggests that lipid membrane was not markedly implicated in this alteration.

Because the adhering of the intracellularly produced globins to the MS spectrin network has been shown as the prime reason for the PHZ-induced stiffening of RBCs (Reinhart et al. 1986), the same physical contact of globins with the spectrin filaments could be assumed to be the prime cause for the accompanying inhibition of the dielectric relaxations of spectrin. To test this possibility, similar experiments were carried out with H_2O_2 that exhibits similar mechanism for generation of globins that rigidify the spectrin filaments and RBC membrane.

Effect of H_2O_2

H_2O_2 is water-soluble oxidant that permeates the cell membrane and rapidly enters the cytoplasm. Several studies have reported that *in vitro* oxidation of whole RBCs by H_2O_2 resulted in dose-dependent increase in echinocyte formation, membrane rigidification and commensurate impairment of RBC deformability (Snyder et al. 1985; Fortier et al. 1988; Hebbel et al. 1990; Schrier and Mohandas 1992; Hale et al. 2011). Although some lipid peroxidation was also observed, it was shown that the major changes in membrane rigidity were primarily due to the formation of complexes between spectrin filaments and the globins of oxidized hemoglobin (Snyder et al. 1985). The morphologic changes and membrane rigidification of H_2O_2-treated RBCs have been both found closely correlated with the extent of spectrin-globin linking (Snyder et al. 1985). In addition, the produced globin-spectrin complexes affected spectrin network organization and caused clustering and reduced mobility of band 3 integral protein, that constitute the antigenic determinate for recognition and removal of senescent cells (Low et al. 1985; Snyder et al. 1985; Fortier et al. 1988; McPherson et al. 1992; Kiefer et al. 1995). Here, the alteration of RBCs by H_2O_2 was carried out at the same experimental conditions (hematocrit value and H_2O_2 concentrations) as those used to test the effect of H_2O_2 on the deformability of RBCs (Snyder et al. 1985).

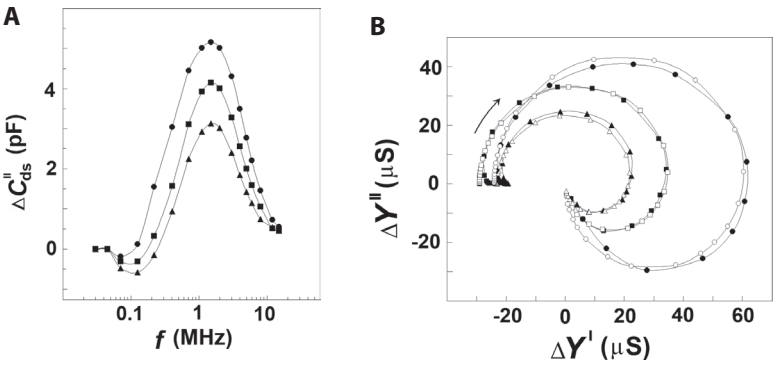

Figure 6. Effect of H_2O_2 on the dielectric relaxations on the MS spectrin of RBCs. Dielectric loss curve of the MS spectrin (**A**) and plot of spectrin-linked portion of the complex admittance (**B**) of H_2O_2-treated RBCs. Suspension contained control RBCs (●, ○) and RBCs treated by H_2O_2 at concentrations 150 μM (▪, □), 300 μM (▲, Δ) and 450 μM (♦, ◊). Other details as for Figure 1.

Up to 450 μM, H_2O_2 produced concentration-dependent inhibition of β_{sp} and $\gamma1_{sp}$ relaxations, as shown in the ΔY" *vs.* ΔY' plot (Fig. 6B), and of β_{sp} relaxation, as shown in the plot of dielectric loss curve of MS spectrin (Fig. 6A). For each concentration of H_2O_2, the model complex admittance plot and the values of the capacitive and resistive elements of the model circuit are shown in Figure 6B and Table 5, respectively. These data substantiate that the inhibitory effect of H_2O_2 on the strengths of the two dielectric relaxations correlates, according to (Snyder et al. 1985; Fortier et al. 1988; Hebbel et al. 1990; Schrier and Mohandas 1992; Hale et al. 2011), to the accompanying stiffening effect of this reagent on the RBC plasma membrane.

Discussion

In this study several stress-inducing chemical agents; DTT, NEM, saponins, PHZ and H_2O_2, were applied on human RBCs. The effects produced by these agents on the dielectric activity of MS spectrin in radio frequency range were compared to the effects they produced on RBC deformability known from other reports. Nevertheless, that these agents display different targets and mechanisms of action, the final effect on the dielectric activity of MS spectrin correlated the known effect they produced on the deformability of RBC plasma membrane. As in other study (Ivanov and Paarvanova 2019a), this outcome again implicates the dielectric activity and related intramolecular mobility of MS spectrin in the mechanism of RBC membrane deformability.

More specific insight into this implication could be derived from the results obtained with PHZ and H_2O_2. These results indicate that both PHZ and H_2O_2 inhibited the dielectric relaxations of spectrin network at the same concentrations whereat they are known, according to (Snyder et al. 1985; Reinhart et al. 1986), to impair the deformability of RBC membrane by generating globin-spectrin complexes. These findings pointed out to the formation of globin-spectrin complexes as a possible common reason for both the impairment of membrane deformability and inhibition of dielectric relaxations of spectrin.

Above lines of evidence suggest that the dielectric activity of MS spectrin in radio-frequency range and the deformability of spectrin network could be both associated with some distinct, dielectric-active and commensurate with the globins of denatured hemoglobin, segments of spectrin filament. The chemical groups and/or side chains of the backbone of spectrin monomer must be excluded as they are much smaller by size than the globin and their dielectric activity is manifested at much higher frequencies (Asami 2015; Gimsa 2017). Above assumption is substantiated by the modern concept that intramolecular flexibility of spectrin filaments strongly contributes to the RBC membrane deformability (Mohandas and Gallagher 2008).

In addition to above considerations, recent studies (Ivanov and Paarvanova 2016; Ivanov et al. 2020) have presented data in support of the possibility that the triple-helical repeat units of spectrin monomer could be the assumed dielectric-active globin-sized segments. Indeed, depending on the deformation of RBC, the linker region between two triple-helical repeat units is able to bend in different angles up to 90° (Brown et al. 2015) while, at the same time, the mere triple-helical repeat units preserve their rod-like shape. Due to their non-compensated dipole moment and large molecular weight of about 11.6 kDa, the triple-helical repeat units could demonstrate dielectric activity in the radio-frequency region. On the other hand, the binding of a given intracellularly generated globin (molecular weight about 16 kDa) to such segment would strongly quench its dielectric activity in the radio frequency region although that of its chemical groups and side chains could be preserved. Compared to the repeat units of spectrin filament the linker regions between them are more flexible hence, the immobilization of a given repeat unit could not be transmitted to the neighbor repeat units. Thus, in line with the data of Reinhart et al. (1986), the formation of discrete complexes, each containing repeat unit and globin(s), would cause focal immobilization until these complexes cover the entire cell endoface producing overall membrane rigidification.

Conclusion

Combined with selective heat denaturation of spectrin, the electro-impedance spectroscopy revealed two relaxations from the spectrin-linked dielectric properties of human

Table 5. Model parameters of β_{sp} and $\gamma1_{sp}$ dielectric relaxations on the MS spectrin of RBCs, pre-treated by H_2O_2

H_2O_2 (μM)	C_0 (pF)	Y_0 (μS)	$-Y_{\beta sp}$ (μS)	$-C_{\beta sp}$ (pF)	$Y_{\gamma1sp}$ (μS)	$C_{\gamma1sp}$ (pF)	$-Y_{\gamma1sp}/Y_{\beta sp}$	$-C_{\gamma1sp}/C_{\beta sp}$
0	37	61	113	12.0	89	1.6	0.788	0.131
150	35	85	79	10.1	50	0.9	0.633	0.088
450	27	105	55	7.0	32	0.6	0.582	0.081

Other details as for Figure 6 and Table 1.

erythrocytes. Specific modifications of spectrin, which impair the deformability of erythrocyte membrane, have been shown to inhibit these relaxations. The inhibition of these relaxations, caused by N-ethylmaleimide, depended on whether the RBCs were swelled or shrunk indicating that the number of accessible SH-groups on spectrin was a function of membrane deformation. In addition, these relaxations were inhibited by nano particles (globins of denatured hemoglobin), generated within the cytosol, known to cross-link and rigidify spectrin. Thus, the differential thermal dielectroscopy at the spectrin denaturation temperature appears as promising technique to provide additional insight into the alterations of the spectrin network that affect the mechanical function of erythrocyte plasma membrane.

References

Abdalla S (2011): Effect of erythrocytes oscillations on dielectric properties of human diabetic-blood. AIP Advances **1,** 012104 https://doi.org/10.1063/1.3556986

Abdalla S, Al-ameer SS, Al-Magaishi SH (2010): Electrical properties with relaxation through human blood. Biomicrofluidics **4,** 034101 https://doi.org/10.1063/1.3458908

Almeida JP, Carvalho FA, Freitas T, Saldanha C (2008): Modulation of hemorheological parameters by the erythrocyte redox thiol status. Clin. Hemorheol. Microcirc. **40,** 99-111 https://doi.org/10.3233/CH-2008-1120

Arduini A, Storto S, Belfiglio M, Sourti R, Mancinelli G, Federici G (1989): Mechanism of spectrin degradation induced by phenylhydrazine in intact human erythrocytes. Biochim. Biophys. Acta **979,** 1-6 https://doi.org/10.1016/0005-2736(89)90515-4

Asami K (2015): Radiofrequency dielectric properties of cell suspensions. In: Dielectric Relaxations in Biological Systems. Physiscal Principles, Methods, and Applications (Eds. V Raicu and Y Feldman), pp. 340-362, Oxford University Press https://doi.org/10.1093/acprof:oso/9780199686513.003.0013

Barbarino F, Wäschenbach L, Cavalho-Lemos V, Dillenberger M, Becker K, Gohlke H, Cortese-Krott MM (2020): Targeting spectrin redox switches to regulate the mechanoproperties of red blood cells. Biol. Chem. **402,** 317-333 https://doi.org/10.1515/hsz-2020-0293

Batyuk LV, Kizilova N (2018): Modeling of dielectric permittivity of the erythrocyte membrane as a three-layer model. In: Development trends in medical science and practice: the experience of countries of Eastern Europe and prospects of Ukraine (Eds. LV Batyuk and N Kizilova), pp. 18-37, Baltija Publishing, Riga https://doi.org/10.30525/978-9934-571-31-2_2

Baumann E, Stoya G, Völkner A, Richter W, Lemke C, Linss W (2000): Hemolysis of human erythrocytes with saponin affects the membrane structure. Acta Histochem. **102,** 21-35 https://doi.org/10.1078/0065-1281-00534

Becker PS, Cohen CM, Lux SE (1986): The effect of mild diamide oxidation on the structure and function of human erythrocyte spectrin. J. Biol. Chem. **261,** 4620-4628 https://doi.org/10.1016/S0021-9258(17)38547-2

Blanc L, Salomao M, Guo X, An X, Gratzer W, Mohandas N (2010): Control of erythrocyte membrane-skeletal cohesion by the spectrin-membrane linkage. Biochemistry **49,** 4516-4523 https://doi.org/10.1021/bi1003684

Brandts JF, Erickson L, Lysko K, Schwartz AT, Taverna RD (1977): Calorimetric studies of the structural transitions of the human erythrocyte membrane. The involvement of spectrin in the A transition. Biochemistry **16,** 3450-3454 https://doi.org/10.1021/bi00634a024

Brown JW, Bullitt E, Sriswasdi S, Harper S, Speicher DW, McKnight CJ (2015): The physiological molecular shape of spectrin: a compact supercoil resembling a Chinese finger trap. PLoS Comput. Biol. **11,** 1004302 https://doi.org/10.1371/journal.pcbi.1004302

Chasis JA, Mohandas N (1986): Erythrocyte membrane deformability and stability: Two distinct membrane properties that are independently regulated by skeletal protein associations. J. Cell Biol. **103,** 343-350 https://doi.org/10.1083/jcb.103.2.343

de Oliveira S, Saldanha C (2010): An overview about erythrocyte membrane. Clin. Hemorheol. Microcirc. **44,** 63-74 https://doi.org/10.3233/CH-2010-1253

Desouky OS (2009): Rheological and electrical behavior of erythrocytes in patients with diabetes mellitus. Romanian J. Biophys. **19,** 239-250

Ferru E, Giger K, Pantaleo A, Campanella A, Grey J, Ritchie K, Vono R, Turrini F, Low PS (2011): Regulation of membrane-cytoskeletal interactions by tyrosine phosphorylation of erythrocyte band 3. Blood **117,** 5998-6006 https://doi.org/10.1182/blood-2010-11-317024

Fischer TM, Haest CWM, Stöhr M, Kamp D, Deuticke B (1978): Selective alteration of erythrocyte deformability by SH-reagents evidence for an involvement of spectrin in membrane shear elasticity. Biochim. Biophys. Acta **510,** 270-282 https://doi.org/10.1016/0005-2736(78)90027-5

Fortier N, Snyder LM, Garver F, Kiefer C, McKeney J, Mohandas N (1988): The relationship between in vivo generated hemoglobin skeletal protein complex and increased red cell membrane rigidity. Blood **71,** 1427-1431 https://doi.org/10.1182/blood.V71.5.1427.1427

Francis G, Kerem Z, Makkar HP, Becker K (2002): The biological action of saponins in animal systems: a review. Br. J. Nutr. **88,** 587-605 https://doi.org/10.1079/BJN2002725

Frenkel N, Makky A, Sudji IR, Wink M, Tanaka M (2014): Mechanistic investigation of interactions between steroidal saponin digitonin and cell membrane models. J. Phys. Chem. B **118,** 14632-14639 https://doi.org/10.1021/jp5074939

Gabriel S, Lau RW, Gabriel C (1996): The dielectric properties of biological tissues: II. Measurements in the frequency range 10 Hz to 20 GHz. Phys. Med. Biol. **41,** 2251-2269

https://doi.org/10.1088/0031-9155/41/11/002
Gimsa J (2017): Electric and magnetic fields in cells and tissues. In: Reference Module in Materials Science and Materials Engineering (Ed. S Hashmi), pp. 1-10, Oxford, Elsevier https://doi.org/10.1016/B978-0-12-803581-8.00982-6
Go YM, Chandler JD, Jones DP (2015): The cysteine proteome. Free Radic. Biol. Med. **84,** 227-245 https://doi.org/10.1016/j.freeradbiomed.2015.03.022
Hale JP, Winlove CP, Petrov PG (2011): Effect of hydroperoxides on red blood cell membrane mechanical properties. Biophys. J. **101,** 1921-1929 https://doi.org/10.1016/j.bpj.2011.08.053
Hebbel RP, Leung A, Mohandas N (1990): Oxidation-induced changes in microrheologic properties of the red blood cell membrane. Blood **76,**1015-1020 https://doi.org/10.1182/blood.V76.5.1015.1015
Ivanov IT, Paarvanova BK (2016): Dielectric relaxations on erythrocyte membrane as revealed by spectrin denaturation. Bioelectrochemistry **110,** 59-68 https://doi.org/10.1016/j.bioelechem.2016.03.007
Ivanov IT, Paarvanova BK (2019a): Thermal dielectroscopy study on the vertical and horizontal interactions in erythrocyte submembrane skeleton. Electrochim. Acta **317,** 289-300 https://doi.org/10.1016/j.electacta.2019.05.159
Ivanov IT, Paarvanova BK (2019b): Effect of permeant cryoprotectants on membrane skeleton of erythrocytes. Probl. Cryobiol. Cryomed. **29,** 237-245 https://doi.org/10.15407/cryo29.03.237
Ivanov IT, Paarvanova BK, Tacheva BT, Slavov T (2020): Species-dependent variations in the dielectric activity of membrane skeleton of erythrocytes. Gen. Physiol. Biophys. **39,** 505-518 https://doi.org/10.4149/gpb_2020034
Ivanov IT, Paarvanova BP (2021): Differential dielectroscopic data on the relation of erythrocyte membrane skeleton to erythrocyte deformability and flicker. Eur. Biophys. J. **50,** 69-86 https://doi.org/10.1007/s00249-020-01491-4
Johnson CP, Tang HY, Carag C, Speicher DW, Discher DE (2007): Forced unfolding of proteins within cells. Science **317,** 663-666 https://doi.org/10.1126/science.1139857
Kiefer CR, Trainor JF, McKenney JB, Valeri CR, Snyder LM (1995): Hemoglobin-spectrin complexes: interference with spectrin tetramer assembly as a mechanism for compartmentalization of band 1 and band 2 complexes. Blood **86,** 366-371 https://doi.org/10.1182/blood.V86.1.366.bloodjournal861366
Low PS, Waugh SM, Zinke K, Drenckhahn D (1985): The role of hemoglobin denaturation and band 3 clustering in red blood cell aging. Science **227,** 531-533 https://doi.org/10.1126/science.2578228
Macdonald JR, Johnson WB (2005): Fundamentals of impedance spectroscopy. In: Impedance Spectroscopy: Theory, Experiment, and Applications (Eds. E Barsoukov and JR Macdonald), pp. 1-26, John Wiley & Sons, Inc https://doi.org/10.1002/0471716243.ch1
McPherson RA, Sawyer WH, Tilley L (1992): Rotational diffusion of the erythrocyte integral membrane protein band 3: effect of hemichrome binding. Biochemistry **31,** 512-518 https://doi.org/10.1021/bi00117a030
Mohandas N, Chasis JA, Shohet S (1983): The influence of membrane skeleton on red cell deformability, membrane material properties and shape. Semin. Hematol. **20,** 225-242
Mohandas N, Gallagher PG (2008): Red cell membrane: past, present, and future. Blood **112,** 3939-3948 https://doi.org/10.1182/blood-2008-07-161166
Pethig R (1979): Dielectric and Electronic Properties of Biological Materials. John Wiley & Sons
Ramot Y, Koshkaryev A, Goldfarb A, Yedgar S, Barshtein G (2008): Phenylhydrazine as a partial model for beta-thalassaemia red blood cell hemodynamic properties. Br. J. Haematol. **140,** 692-700 https://doi.org/10.1111/j.1365-2141.2007.06976.x
Rangachari K, Beaven GH, Nash GB, Clough B, Dluzewski AR, Myint-Oo, Wilson RJ, Gratzer WB (1989): A study of red cell membrane properties in relation to malarial invasion. Mol. Biochem. Parasitol. **34,** 63-74 https://doi.org/10.1016/0166-6851(89)90020-0
Reinhart WH, Sung LA, Chien S (1986): Quantitative relationship between heinz body formation and red blood cell deformability. Blood **68,** 1376-1383 https://doi.org/10.1182/blood.V68.6.1376.1376
Saldanha C, de Almeida JPL, Freitas T, Oliveira S, Silva-Herdade AS (2010): Erythrocyte deformability responses to shear stress under external and internal stimuli influences. Series on Biomechanics **25,** 54-60
Schrier SL, Mohandas N (1992): Globin-chain specificity of oxidation-induced changes in red blood cell membrane properties. Blood **79,** 1586-1592 https://doi.org/10.1182/blood.V79.6.1586.1586
Seeman P, Cheng D, Iles FH (1973): Structure of membranes holes in osmotic and saponin hemolysis. J. Cell Biol. **56,** 519-527 https://doi.org/10.1083/jcb.56.2.519
Sheetz MP (1983): Membrane skeletal dynamics: role in modulation of red cell deformability, mobility of transmembrane proteins, and shape. Semin. Hematol. **20,** 175-188
Sheremet'ev IA, Sheremet'eva AV (2009): Effect of dithiothreitol on the deformation and La(3+)-induced fusion of human erythrocytes. Biofizika **54,** 249-251 https://doi.org/10.1134/S0006350909020092
Simeonova M, Wachner D, Gimsa J (2002): Cellular absorption of electric field energy: influence of molecular properties of the cytoplasm. Bioelectrochemistry **56,** 215-218 https://doi.org/10.1016/S1567-5394(02)00010-5
Sleep J, Wilson D, Simmons R, Gratzer W (1999): Elasticity of the red cell membrane and its relation to hemolytic disorders: An optical tweezers study. Biophys. J. **77,** 3085-3095 https://doi.org/10.1016/S0006-3495(99)77139-0
Snyder LM, Fortier NL, Trainor J, Jacobs J, Lob L, Lubin B, Chiu D, Shohet S, Mohandas N (1985): Effect of hydrogen peroxide exposure on normal human erythrocyte deformability, morphology, surface characteristics, and spectrin-hemoglobin cross-linking. J. Clin. Invest. **76,** 1971-1977 https://doi.org/10.1172/JCI112196
Speicher DW, Davis G, Marchesi VT (1983): Structure of human erythrocyte spectrin. II. The sequence of the a-I domain. J. Biol. Chem. **258,** 14938-14947 https://doi.org/10.1016/S0021-9258(17)43754-9

Winter WP (1994): Mechanism of saponin induced red cell hemolysis: Evidence for the involvement of aquaporin CHIP28. Blood **84,** Abstr. 445

Yoshino H, Minari O (1987): Heat-induced dissociation of human erythrocyte spectrin dimer into monomers. Biochim. Biophys. Acta **905,** 100-108 https://doi.org/10.1016/0005-2736(87)90013-7

Received: July 15, 2021
Final version accepted: December 26, 2021